# Flow Phenomena in Compressor Casing Treatment

G. D. J. Smith[1]

N. A. Cumpsty

Whittle Laboratory,
Department of Engineering,
University of Cambridge,
Cambridge CB3 0EL, England

An axial skewed slot casing treatment has been tested over the tips of an isolated low-speed rotor with a hub-tip ratio of 0.4. An improvement in stall margin of 22 percent at nominal clearance was obtained. Detailed measurements of the loss pattern downstream of the rotor were made with a hot wire. Measurements were also made in the blade passage with a traversing gear moving with the rotor and in the treatment slots themselves using hot wires. The tentative conclusion is that unsteady effects in the slot are of secondary importance. Of primary importance is the selective removal of high absolute swirl, high loss fluid from the endwall near the trailing edge of the pressure surface of the blade, and reintroduction of this, with absolute swirl direction reversed, near the blade leading edge.

## Introduction

In the late 1960s, it was discovered that the stall of a compressor could be delayed to smaller mass flows by having treatment over the rotor tips. Since then, many different geometries of treatmant have been tested, for example [1-12]. Such treatments can only be useful if the compressor is taken into stall by the rotor tips (i.e., is "tip critical") or stator hub, but with this proviso a large number of different treatment geometries have been found to be effective. It also appears from these tests that the flow Mach number is not critical to the behavior of the treatment, similar improvements in stall margin being produced by a given treatment at tip Mach number of, for example, 1.5 and 0.15.

The different treatments are not all equally effective. Perhaps the most successful treatment for reducing the mass flow at stall is the axial skewed slot, and this is the treatment used for the experiments described here. (The geometry is shown in Fig 1 and described more fully in section on the axial flow compressor rig.) An essential feature of the design is the inclination of the slots so that flow emerging from them would possess swirl in the opposite sense to the rotor motion. Tests by Takata and Tsukuda [2] showed that if the inclination was reversed (so that flow emerged from the slots in the rotor direction) the compressor actually stalled at a higher mass flow rate than with a solid wall.

Despite the usefulness of casing treatment for extending the unstalled operating range of compressors, it has so far found fairly limited application. One major reason for this is that the treatments most effective in extending the range usually degrade the efficiency significantly.

A treatment that will break away from this constraint would be most valuable, but a systematic approach to obtaining this requires that there should first be a good understanding of the way in which existing casing treatments

operate. Most of the many past tests on treatments have looked at the effect of the treatment on the flow leaving the rotor without investigating the flow phenomena occurring in and just above the treatment, but a few, notably by Prince et al. [1], Camarata et al. [3], and Takata and Tsukuda [2], did examine the flow inside the slots grooves of the treatment. As expected, flow entered the slots near their rear and reemerged near the front where the static pressure was low. Greitzer et al. [4] showed detailed downstream profiles of relative total pressure that allowed some interpretation of the processes. The present paper describes measurements taken behind the rotor, inside the slots, and between the moving blades. From this base, most of the processes occuring can be regarded as well determined, but it must be admitted that there are aspects of the flow behavior which are not properly understood.

Part of the difficulty in understanding the operation of the treatment is the ignorance surrounding the cause of stall in even a smooth wall (i.e., no casing treatment) compressor. The most conventional view is that rotating stall is initiated by a separation from the surface of the blades; because of the high-incidence into the rotor in the annulus boundary layer separation is likely to occur first for the rotor near the casing. This view of the process of stall underpins the tentative explanation of casing treatment behavior presented by Mikoljczak and Pfeffer [5]. This was based on flow visualization experiments using a linear cascade in water with a grooved belt moving past the blade tips.

The experimental data obtained with the smooth walled build of the compressor used for the tests described here do not show any tendency for stall to be initiated on the suction side, but on the contrary, the region of low relative total pressure fluid collects by the pressure surface. This tendency, which is explainable in terms of the inlet skew and the tip clearance flow, is demonstrated below but is mentioned here to draw attention to the difference of opinion regarding stall inception.

Greitzer et al. [4] conducted a carefully thought-out experiment based on the hypothesis that stall could be initiated either on the annulus wall or on the blade. It was postulated
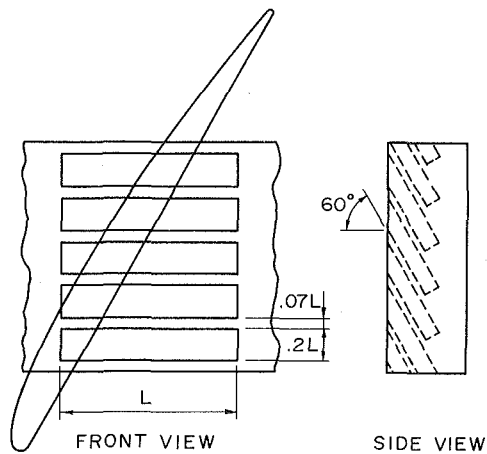
---

**Fig. 1 Axial skewed slot treatment**

that casing treatment would be effective in improving the range for the former but not the latter. The blade loading was increased (in order to produce blade stall) by removing every other blade so that the diffusion factor exceeded the normally permitted value. The hypothesis was apparently borne out very closely; a large improvement in range was produced for the high solidity blades for which the cascade diffusion factor limits were not exceeded, but no effect on stall margin was produced for the more highly loaded blades. It should be remarked that these blades were quite highly cambered (49 deg at the tip) and different behavior to that observed with low camber, high-stagger fan tip sections might be expected. The smooth walled build of low solidity showed no accumulation of loss near the pressure face of the blades but a large accumulation near the suction side. The high-solidity smooth walled build does show the loss towards the pressure side in a manner not very dissimilar to that on the present fan tip.

A recent paper by Koch [13] has succeeded in correlating stalling pressure rise for a very wide range of compressors assuming that the stalling process occurs on the endwall. Blade stall in the sense of the paper by Greitzer et al. [4] is also likely to occur close to the endwall where the incidence is high. The failure of the casing treatment to delay stall in this case appears to be contrary to the ideas presented by Mikoljczak and Pfeffer [5], who suggested that the casing treatment has its beneficial effect by drawing flow from the suction surface corner.

The confusion surrounding the process of stalling will help to explain the difficulty encountered in explaining the process even with the detailed and interlocking sets of measurements described in the present paper.

## The Axial Flow Compressor Rig

An existing low-speed compressor of 1.52-m tip diameter and 0.4 hub/tip ratio was used throughout the experimental program. The research rotor was fitted with 22 blades of constant chord length 152.4 mm, giving hub and tip solidities

of 1.43 and 0.47, respectively. The overall features of the rig and blading have already been described by Gregory-Smith [14]. The rotor is designed for a free-vortex flow at a flow coefficient of 0.70. The rotor tips are staggered at 60.7 deg with 7.8 deg of camber, C4 section and 8 percent thickness/chord ratio.

A 4:1 contraction ratio bellmouth formed the entry to the compressor, and this housed screens and an aluminum honeycomb flow straightener to minimize large scale flow nonuniformities. Inlet guide vanes and stators were not used, but the research rotor was run in series with an auxiliary fan positioned far downstream of the working area. Speed control on both rotors and a variable position throttle in the exhaust permitted a wide range of flow conditions to be obtained.

The treatment was the same design that Prince et al. [1] had tested, which in turn had been based on data gathered from early NASA work [6, 9]. The treatment, shown in Fig. 1, had rectangular cavities that extended axially over the middle 73 percent of the axial chord. The length of the slot, 55 mm, was five times greater than its breadth, and the depth was half the length. Like Prince's design, the depth of the slot was inclined at 60 deg to the radial in such a way that flow emerging from the slot would do so with swirl contrary to the blade direction. The slot design gave an open area to total area ratio of approximately 0.70.

## Flow Measuring Equipment

A full description of the instrumentation and the measurement technique is given by Smith [15]. Radial traverses were made downstream of the rotor blades (and in a few cases upstream) using a conventional three-hole cobra probe. The probe was operated in the null-yaw mode to give flow angle and total pressure. High-frequency response measurements were taken with constant temperature hot wires and flush mounted transducers. An angled hot-wire technique, as employed by Whitfield et al. [16], was used downstream of the blade row, where the three-dimensional character of the flow was of interest. This technique can only be used in situations where the range of flow angle is known to fall within the calibration of the probe; the calibration cannot be extended to cover all flow angles, as the support pins then fall upstream of the hot wire introducing errors due to shielding. The angled hot wire was therefore not suited to flow measurements inside the treatment slots where the flow direction could vary by 180 deg. Instead a shielded hot wire, entering through the side of the slot, was used to find the velocity direction and sense, and a separate conventional hot wire, entering through the bottom of the slot, was used to measure the flow velocity. This latter probe had 20-mm-long pins supporting the wire to minimize the effects of flow blockage. The wire was aligned normal to the slot length and normal to the compressor axis.

A computerized data acquisition system was used for all the hot wire and high-response pressure transducer tests. With this system, the rapidly varying input signals could be phase locked to a physical event, in this case determined by a particular blade passing over a magnetic trigger.

For an understanding of how the treatment improved flow

## Nomenclature

| | |
|---|---|
| $C_s$ = flow velocity in treatment slot | $CT$ = casing treatment build |
| $C_t$ = tangential component of absolute flow velocity | $P_o$ = total pressure |
| | $P_s$ = static pressure |
| $C_x$ = axial component of fluid velocity | SW = smooth wall build |
| | $t/c$ = blade tip clearance to chord ratio |

$U_m$ = Midspan blade speed
$U_t$ = tip blade speed
$\beta_2$ = absolute outlet flow angle
$\psi_{ss}$ = $\Delta P_s/\frac{1}{2}\rho U_m^2$, nondimensional static pressure rise across rotor
$\phi$ = flow coefficient, $C_{x/U_M}$

stability, it was important to measure the velocity and pressure in between the rotor blades and close to the casing treatment. These measurements were taken with a 5-hole probe rotating with the rotor. The probe was operated in the fixed direction mode and probe pressures were transferred to the stationary frame via a sealed-bearing, pressure-transfer device. These data were processed using a technique developed by Lewis [17] to give the total and static pressures and the three velocity components. This rotating frame probe traversed a surface bordered by the blade pressure and suction surfaces and by the passage leading and trailing edges. After such a surface had been traversed, it was necessary to stop the rig in order to move the probe to a new radial position. By repeating this process, a three-dimensional picture of the flow in the rotating passage of the blade could be developed; traverses taken at five different radial surfaces gave an adequate definition of the flow.



**Fig. 2 Static pressure rise characteristics at various tip clearances for the solid wall and treated builds**

## Compressor Characteristics

Figure 2 shows nondimensional static-to-static pressure rise against nondimensional flow rate for smooth wall (sw) and casing treatment (ct) builds at a range of tip clearances expressed as a percentage of blade chord. In low-speed tests, stall margin improvement is commonly expressed as the percentage reduction in the mass flow rate just prior to stall which accompanies the fitting of the treatment. With this definition, a stall margin improvement of 21.7 percent is obtained at nominal clearance, i.e., $t/c = 1$ percent.

It is well known that increasing the blade tip clearance reduces the pressure rise and prematurely precipitates the stall. From this point of view the increase in flow area beneath the blade tips that is associated with the geometry of the treatment slots might be expected to exacerbate this loss in performance. In practice, this was not the case and substantial improvements in flow range were achieved in high tip clearance builds. The results presented in Fig. 2 show stall margin improvement to increase with tip clearance from a value of 21.7 percent at nominal clearance to 28 percent at 6 percent clearance. (The absence of a pressure discontinuity on the curve for the build of largest clearance, $t/c = 11$ percent, precludes an exact calculation of stall margin improvement, but an improvement of 20 percent is obtained at peak pressure rise.) It is noteworthy that the tip clearance of the treated rig could be increased by 5 mm (to $t/c = 3.5$ percent) without the outlet pressure dropping below the peak value realized with the solid wall compressor. It seems possible that the ability of the casing treatment to minimize the deleterious effects of tip clearance may recommend its use even more than its ability to reduce the flow at stall with nominal clearance.

The results in Fig. 2 indicate that treating the compressor has lead to a significant increase in the pressure rise just prior to the stall, but it can also be seen that the treatment has little effect on the characteristic at high flow rates near the free vortex design point. In addition, the Reynolds number dependence of the compressor unstalled behavior is slight, with the nondimensional pressure rise characteristics being almost independent of rotor speed over a factor of two. All subsequent results shown in this paper are therefore only for a single rotational speed of 450 rev/min, and these results always apply to the nominal clearance of 1 percent.

The flow behavior just prior to stall in the untreated build ($\phi = 0.4$) differed markedly from that found in the treated case at the same flow rate. The untreated rig showed a large increase in blockage near the tip critical whereas in the treated rig the only evidence of markedly increased flow blockage occurred near the hub. This information was obtained by
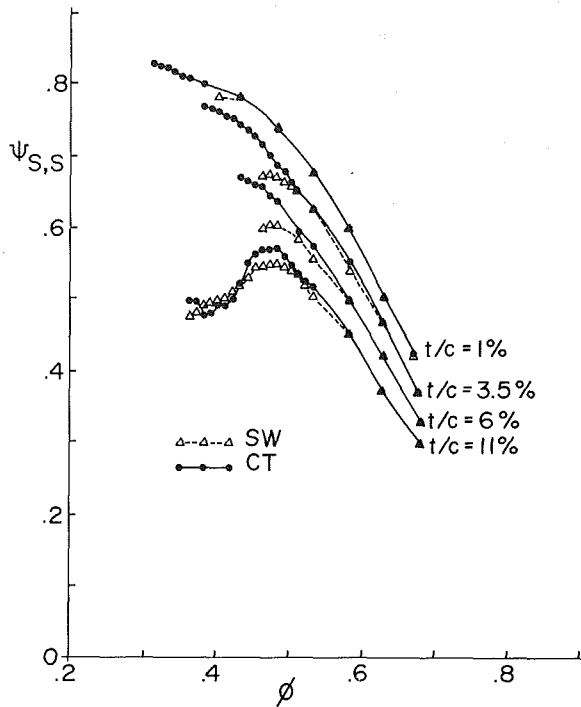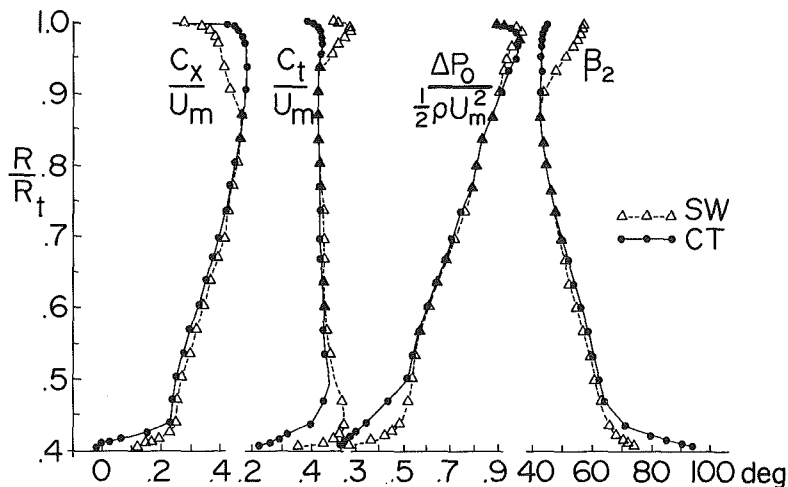


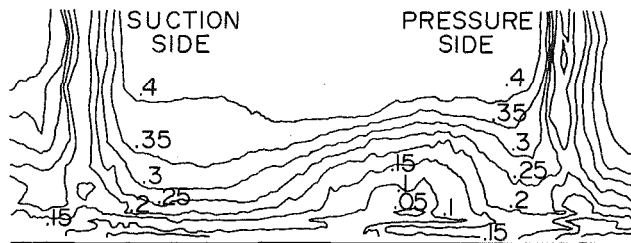**Fig. 3 Outlet flow field for the solid wall and treated builds, $\phi = 0.4$**

**Fig. 4 Axial velocity measured in the radial-tangential plane downstream of the solid wall rotor and nondimensionalized by** $Um$. $\phi = 0.32$
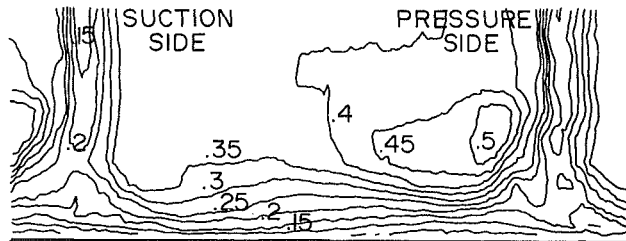


**Fig. 5 Axial velocity measured in the radial-tangential plane downstream of the treated rotor and nondimensionalized by** $Um$. $\phi = 0.32$

simultaneously recording the output from two hot wire probes attached near the hub and tip at identical axial and circumferential stations one axial chord downstream of the rotor. In all cases with the treated outer wall, the hot wire signals showed that a large-scale stalled region completely encircled the hub and covered approximately 10 percent of the span.

Near stall for the treated rig ($\phi = 0.32$) a low-frequency rumble normally characteristic of the presence of rotating stall was emitted, but the hot wire mounted at the hub still showed an axisymmetric pattern of unsteadiness similar to that found at $\phi = 0.4$, although the unsteady flow now extended further along the span. Even though the flow near the hub was unsteady and, close to the hub, even reversed in the axial sense, it should be stressed that the compressor was still operating stably on the unstalled part of the characteristic. Further throttling led to a conventional stall in which the pressure across the rotor dropped abruptly. The reversed or stalled flow that girdled the hub prior to this breakdown was then replaced by a single full-span rotating stall cell and a region of apparently normal flow. The stall cell speed of 0.56 times the rotor speed was unchanged by the presence of the treatment.

It was found that at any given Reynolds number the treated compressor always entered stall at a lower mass flow rate than the untreated build and the mass flow rate at the point of stall recovery was also lower. However, the treated rotor took more time to recover from a rotating stall and the noise from the stalled compressor was more severe than that heard during the stall of the solid wall build. The severity of the stall was difficult to quantify because stall appears over different regions of the pressure rise characteristic of the two builds. Nevertheless, the output from a hot wire showed that the greatest excursions in flow velocity were found during the stall of the treated build.

## Downstream Flow Surveys

The results in Fig. 3 were measured one axial chord downstream of the blade trailing edge using the three hole cobra probe. The two sets of curves in this figure, one for the smooth wall rig and one for the compressor with treatment, were both obtained at a flow coefficient of 0.4, which corresponds to the flow rate marginally greater than that for

stall of the untreated build. Considering the plot of axial velocity, the treatment had the effect of increasing the throughflow in the tip region and decreasing it elsewhere. (This decrease is an indirect influence of the treatment and occurs because treated and solid wall tests were performed at equal overall mass flow rates.) For the treated build, a small region of reversed flow occured near the hub, and flow is probably drawn through the blade passage into the upstream flow field. On this low hub/tip ratio machine the blade outlet angle at the hub is only 1 deg from the axial, and this feature of the free vortex design would make it easier for the direction of flow in the passage to reverse. The reversed flow encircled the hub and reduced the effective annulus through flow area by 1 percent. A conventional hot wire placed 6 mm from the hub and 10 mm downstream of the rotor revealed no clearly defined rotating stall as such, although the flow varied randomly from pitch-to-pitch as if the blades were severely stalled. This axisymmetric unsteadiness covered the first 10 percent of the span but further out the repetitive blade wakes of the normal unstalled flow were found. The extent of the unsteady reversed flow decreased as the throttle was opened until eventually clearly defined blade wakes were found down to the hub. The casing treatment results in Fig. 3 also show a marked reduction in swirl velocity and flow angle in the tip region but remarkably little alteration in total pressure rise.

At the lightly loaded free vortex condition of $\phi = 0.7$ (the flow coefficient for which the rotor was designed), the radial traverse results of the treated and solid wall builds could not be separated, indicating that the treatment is not effective at low-pressure rise conditions. This result may indicate that the efficiency penalty when using treatment as high flow rates is insignificant, but this idea has not been checked.

The velocity surveys made in the tip region with an angled hot wire covered a radial/tangential plane 10 mm downstream of the blade trailing edges. These data are presented as contours of axial velocity for the untreated and treated builds in Fig. 4 and 5 for a flow coefficient of 0.40, the value close to stall for the untreated build. These results were phase locked to the passing blades and slightly more than one blade pitch is shown. For the smooth walled compressor a buildup of low velocity fluid near the blade pressure face is very apparent in Fig. 4. This collection of low axial velocity (and also low velocity relative to the moving blades (Fig. 6)) is attributable to both the effect of inlet skew and, perhaps predominantly, to the flow through the tip clearance. This retarded flow coalesces with a well-defined wake from the blade pressure face. The retarded zone extends over half the blade pitch, but there is no evidence of a buildup of low-velocity fluid near the suction surface.

The traverse for the treated compressor at the same flow rate, Fig. 5, shows completely different features to the solid wall build. Differences are noticed in the pressure face corner, where high axial velocity flow replaces the blockage; in the suction face corner, which is deeply scoured by the free-stream; and all along the annulus wall, where the closely spaced velocity contours show that the boundary layer has been thinned.

Contours of relative dynamic head are shown in Figs. 6 and 7 for the solid wall and treated builds. The low dynamic head region near to the pressure surface is very clear in the untreated compressor but replaced by a region of higher relative total pressure in the treated case.

The cobra probe and the angled hot wire were also used to measure the outlet flow field of the treated compressor at a flow rate just above its stall point. In Fig. 8, cobra probe results of the smooth wall and treated builds are superimposed at flow rates just above their respective stall points ($\phi = 0.4$ and $\phi = 0.32$, respectively). Close to the outer wall the axial velocity profile is very similar in each case and indeed a separate investigation has shown that the axial displacement

thickness is very nearly equal for the two cases. Decreasing the mass flow rate from $\phi = 0.4$ to $\phi = 0.32$ leads to an increase in total pressure, outlet flow angle, and swirl. The increased swirl without significantly increased losses over much of the annulus leads to an increase in the outer wall static pressure, a result consistent with the performance curve shown in Fig. 2, where the static pressure on the outer wall of the treated compressor is seen to increase as the compressor is throttled from $\phi = 0.4$ to $\phi = 0.32$. The reversal of flow near the hub, where the outlet flow angles are in excess of 90 deg, is more pronounced and covers the first 5 percent of the span. The lower values of swirl velocity near the hub follow from the low speed of the reversed flow. The total pressure curve shows that losses have increased in the hub region of the treated build.

Traversing the tip region with an angled hot wire when the treated compressor was operating near to its stalling mass flow rate shows up considerable change in the position of the passage blockage, Fig. 9. This region of low axial velocity is not on the pressure side, as was the case in the smooth wall build, but appears toward the suction side, where it blends in
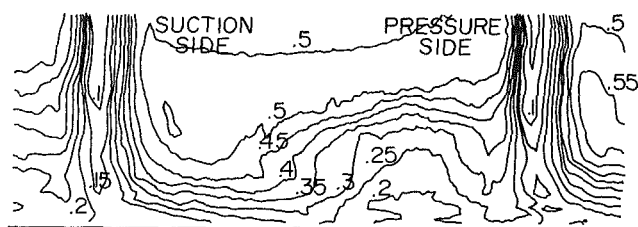
Fig. 6  Relative dynamic head measured in a radial-tangential plane downstream of the solid wall rotor and nondimensionalized by $U_m^2$. $\phi = 0.4$
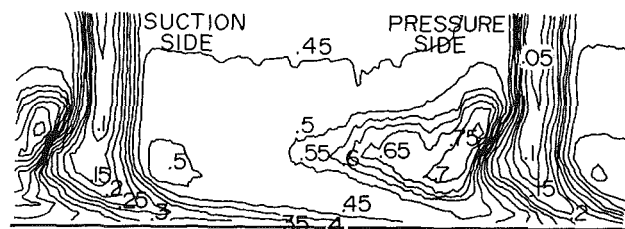
Fig. 7  Relative dynamic head measured in a radial-tangential plane downstream of the treated rotor and nondimensionalized by $U_m^2$. $\phi = 0.32$

with the collosal blade wakes. Considering that stable operation is still maintained in the treated build with this amount of blockage, it is surprising that a lesser blockage on the pressure face of the untreated compressor precipitates its stall. It thus seems that it is the position of the blockage, rather than its magnitude, that is the more crucial precursor to the stall.

The blockage close to the suction surface originates, in part, from blade boundary layer flow on the suction surface streaming down toward the blade tip. This is shown by plotting the hot-wire data in vector form for a flow condition near the stall of the treated compressor, Fig. 10. The vectors represent the resultant of the radial velocity and the projection of axial and tangential velocity components on a plane perpendicular to the blade stagger angle. The blade wakes show up as regions of radial flow streaming down the blade to the outer wall where the flow either integrates with the wall boundary layer or is turned back towards the hub. Flow in the midpitch region is directed towards the hub and vortex like flow patterns are now observed in both blade corners. There is no evidence in the vector plots of flow having moved beneath the blade tip from the pressure face to the suction face. This appears to indicate that the treatment has somehow counteracted the tip leakage flow. This fact could perhaps be inferred from Fig. 2 where the treated compressor performance showed far less degradation because of tip clearance effects than the solid wall compressor. Just to the left of the blade pressure face, the flow shown in Fig. 10 is seen to ride up the blade surfaces as if the blade trailing edge region was performing like a snow plough that scoops up low absolute whirl passage flow. It must be remembered, however, that these measurements were made downstream of the rotor, and as such, they represent the aftermath of the treatment flow.

A vector plot of the outlet flow from the solid wall rig operating near its stall condition is not presented here but these results, [15], showed that the mass flow of boundary layer fluid streaming down the blades was only about a third of that found in the treated build near its stall point. At $\phi = 0.40$, the proportion of the total blockage in the endwall boundary layer that comes from radial flow along the suction surface was calculated by an approximate method in [15] to be less than 4 percent.

Even though the hot-wire technique produced detailed maps of the velocity field downstream of the tip and revealed considerable change in the flow field, it was not possible to explain the high-velocity core in the pressure face corner of
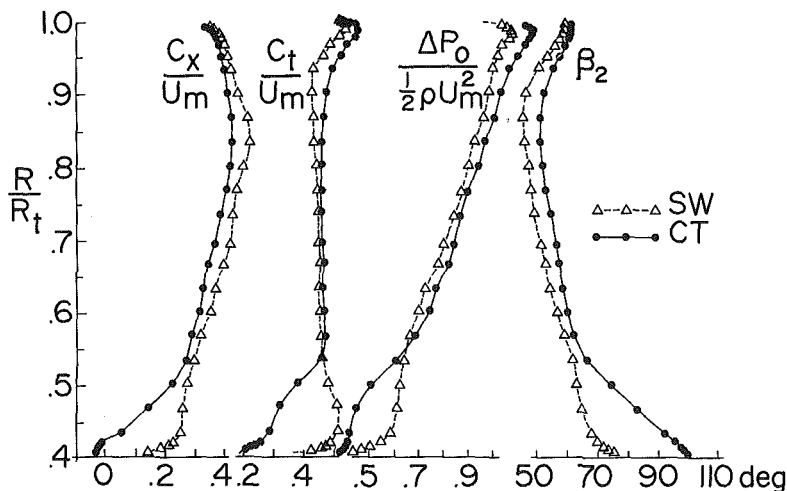
Fig. 8  Outlet flow field for the solid wall and treated builds, $\phi = 0.4$ and $\phi = 0.32$ respectively
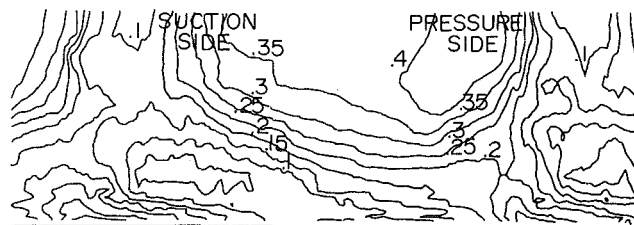
Fig. 9 Axial velocity measured in a radial-tangential plane downstream of the treated rotor and nondimensionalized by $Um$. $\phi$ = 0.32
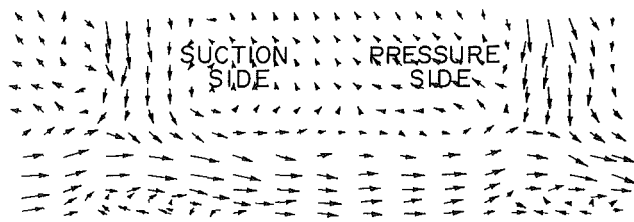


Fig. 10 Relative velocity presented in vectored form for the flow in a radial-tangential plane downstream of the treated rotor, $\phi$ = 0.32
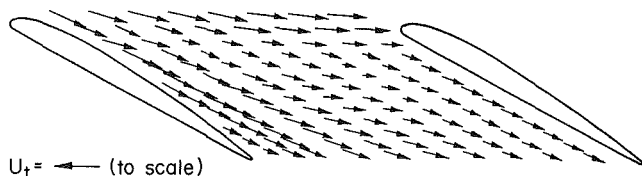


$U_t$ = ◂— (to scale)

Fig. 11 Relative velocity measured in the blade passage 6 mm above the solid wall, $\phi$ = 0.42



Fig. 12 Relative dynamic head measured in the blade passage 6 mm above the solid wall, $\phi$ = 0.42



$U_t$ = ◂— (to scale)

Fig. 13 Absolute velocity field in the blade passage 6 mm above the solid wall, $\phi$ = 0.42

the treated compressor. The interaction of the flow entering and leaving the slot with the flow in the blade passage also remained unknown at this stage.

## Flow in the Rotor Blade Passage

Measurements taken in between the rotor blades with the rotating probe were recorded at flow rates near stall, which were slightly higher than those used in previous tests, since the presence of the rotating probe increased the flow rate at which the compressor stalled.

The first set of results apply to the smooth wall build operating near its stall mass flow, $\phi$ = 0.42, with the traverse plane of the probe being 6 mm above the outer annulus wall. These results are presented in Fig. 11 as a plot of relative flow vectors on a developed plan view of the blade passage. The skewed inlet flow may be seen crossing the blade passage to the pressure face corner as a flow of low relative velocity. This region of flow is shown in Fig. 12 to be part of a stream of low relative dynamic pressure fluid that migrates diagonally across the passage from the vicinity of the suction surface leading edge to approximately the midchord region of the pressure face. It is this cross-passage flow that therefore accounts for the pressure face blockage that was shown in the downstream results, Figs. 4 and 6. The velocity deficit of the inlet annulus wall boundary layers is not in itself the cause of the retarded flow that accumulates in the pressure face corner. In fact, this boundary layer flow enters the blade passage with a relative velocity magnitude no more than a few percent below that of the flow in the freestream. (A simple calculation for a particle entering with vanishingly small axial velocity shows that the relative dynamic pressure cannot be more than 8 percent below that of the freestream.) The boundary layer fluid is thus apparently reenergized by moving into the
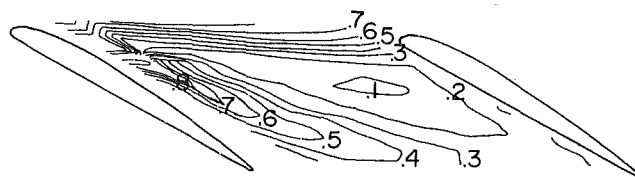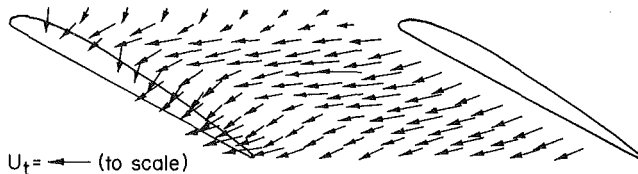
rotating frame. The major cause of the low relative total pressure fluid is probably the tip clearance flow, which is likely to be discharged approximately normal to the blade chord, that is at about 30 deg from the upstream axial direction. In addition, the high skew of the flow increases the blade loading to the extent that there may be flow separation in the blade suction surface/annulus wall corner.

The process becomes clearer when the blade passage results are referred to the absolute frame. Figure 13 is a plot of absolute velocity for the passage flow measured 6 mm from the smooth outer wall at a flow rate of $\phi$ = 0.42. It is noted that the flow always has an absolute swirl component in the same direction as the blade rotation, with the areas of highest swirl appearing at the suction trailing edge and at midpitch position 10 percent of the axial chord from the blade leading edge. The pitch-averaged swirl at the latter position is 0.53 times the blade tip speed and spatially this region of the flow would correspond in the treated compressor to a position directly above the leading edge of the slot.

Measurements taken in the blade passage 6 mm above the treatment at the same flow rate, $\phi$ = 0.42, revealed considerable change in the flow velocity and magnitude. As Fig. 14 shows, the flow near the leading edge of the slot is seen to be pointing 13 deg upstream (measured relative to the tangential direction and averaged over the pitch), and the relative velocity measured in the midpassage above the leading edge of the slot is roughly double that found in the same area of the smooth wall flow. This increase in velocity is most noticeable in the midpassage region where the flow has gained considerably in relative swirl. This flow is toward the pressure surface of the blade where the flow is turned and finally leaves the passage with a velocity 1.5 times greater than that measured in the solid wall build. The high-velocity core previously evident near the pressure surface in Fig. 5 and 7 can be tracked upstream along a roughly diagonal path from the blade pressure face corner at the trailing edge to a region above the leading edge of the slot. It is here that the treatment is ejecting a flow of considerable relative swirl into the blade passage. Figure 14 also shows that the flow in the treated build has the greatest relative swirl just above the leading edge of the slot. The swirl in this region is approximately equal to the blade tip speed of 24 m/s. This is an unexpected result, because flow in the absolute frame above the leading edge of the slots must therefore be almost stationary, see Fig. 16.

The results of the blade passage surveys for the treated wall in absolute coordinates, Fig. 16, show regions of high absolute velocity all along the blade suction surfaces. The flow near the trailing edge of the suction surface has a high absolute velocity because this flow, perhaps a region of

separated flow, has a low relative velocity and therefore a high absolute swirl. It is significant that the region towards the trailing edge of the blades has an absolute flow direction which favors flow entering the skewed axial slots.

The contours of relative dynamic head for the treated build, Fig. 15, do not show the extensive low head region fanning across the passage as they did for the solid wall build, Fig. 12, but towards the trailing edge conditions are comparatively uniform. Near the front of the slot, where flow emerges from it, the contours of dynamic head are more complicated.

The region of almost stagnant flow in the absolute frame is quite extraordinary, since the same region of the flow in the smooth wall build, Fig. 13, has an extremely high absolute swirl (0.5 times the blade tip speed) in the direction of blade rotation. Seemingly the effect of the treatment has been to bring this high absolute flow to a standsill, a result which is expected if flow leaves the leading edge region of the slot with equal and opposite momentum to the flow formerly found in the same region of the smooth wall build. Measurements of static pressure on the annulus walls are presented in Fig. 23 and show that a considerable and localized pressure rise is associated with this deceleration of the flow.

The previous sections considered the data from the blade passage surveys in a surface parallel to the outer annulus wall. Since a number of these surveys were taken at different distances from the outer wall, it is possible to plot these data
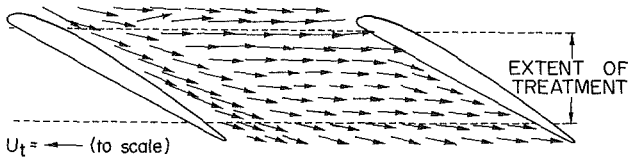


Fig. 14 Relative velocity measured in the blade passage 6 mm above the treated wall, $\phi = 0.34$
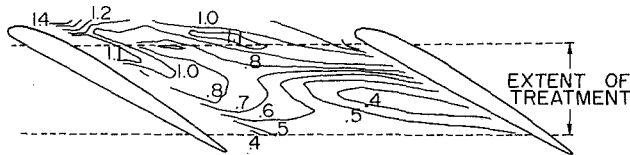


Fig. 15 Relative dynamic head measured in the blade passage 6 mm from the treated wall, $\Phi = 0.34$
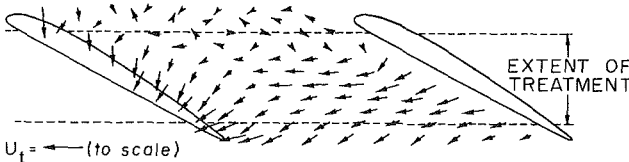


Fig. 16 Absolute velocity field in the blade passage 6 mm above the treated wall, $\phi = 0.34$

in planes parallel to the stagger of the blade to show the nature of the spanwise flows. An example of this is shown in Fig. 17, where vectors are superimposed on a sketch of the blade and treatment. This is for $\phi = 0.42$ and on a plane approximately 25 percent of the pitch from the pressure surface. (Results for the smooth wall build are not shown because the spanwise flows were minimal for this build.) It is apparent that flow is directed towards the treatment over roughly the downstream 60 percent of the passage and away from the treatment over the remaining upstream part of the slot. In fact, these plots show flow directed away from the wall well upstream of the area actually covered by the treatment. It seems that as flow enters the blade passage it is forced to move away from the wall before passing over the jet of fluid emerging from the treatment. Above the downstream half of the treatment slot the flow is drawn towards the treatment; this radial flow direction is maintained downstream of the trailing edge of the treatment slot although the velocity magnitude is then greatly diminished. The flow pattern is only slightly different at other stations in the blade passage, except that in a small area (roughly 5 percent of the passage area) near the leading edge of the suction surface the measurements suggest that flow is directed towards the annulus wall. This finding is examined in detail in [15], where it is concluded that the extremely high shear of the flow in this region leads to unreliable measurement of the radial component of velocity.

When the treated build was operated near to its stall mass flow rate, $\phi = 0.36$, the aforementioned flow features changed in magnitude, but the trends were essentially unaltered.

## Flow Direction and Velocity Within the Slots
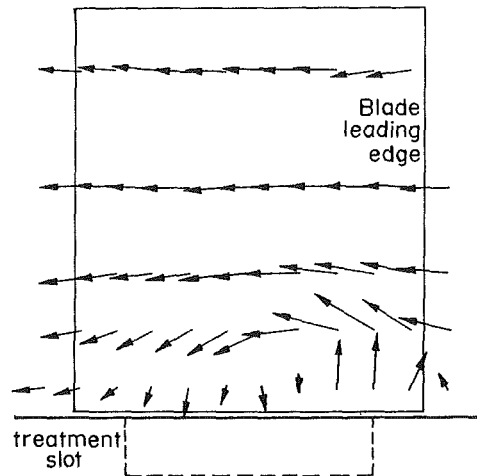
An instantaneous picture of the direction and sense of the



Fig. 17 Spanwise flows in the treated build 20 percent of the pitch from the pressure surface, $\phi = 0.34$
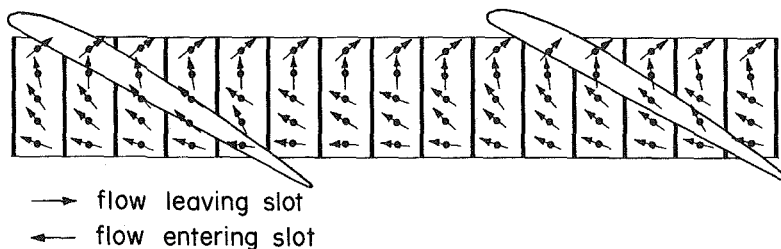


→ flow leaving slot
← flow entering slot

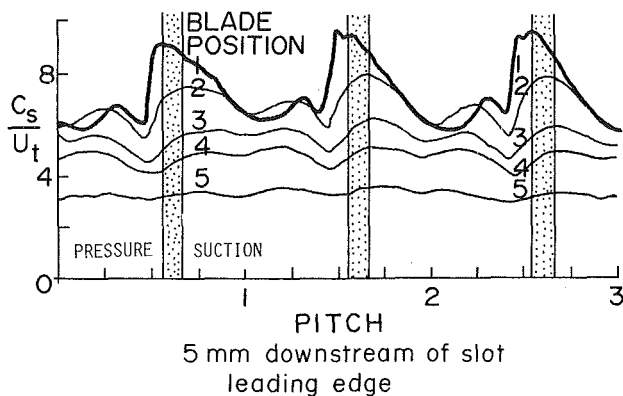Fig. 18 Flow direction at middepth in the treatment slots, $\phi = 0.42$

**Fig. 19 Flow velocity in the treatment slot 5 mm downstream of the slot leading edge, $\phi = 0.42$. Trace 1 is for flow at the treatment lip. Traces 2-5 are at greater depths (i.e., increments of 6.5 mm).**
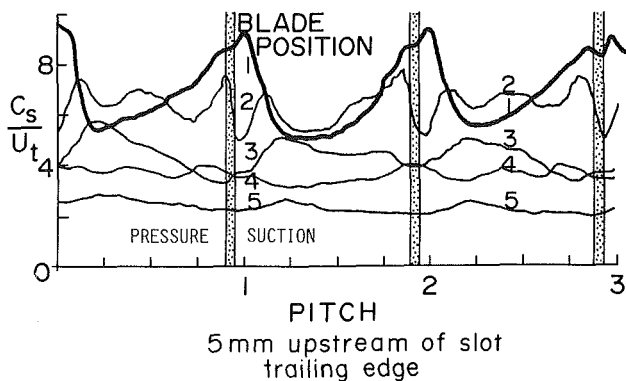


**Fig. 20 Flow velocity in the treatment slot 5 mm upstream of the slot trailing edge, $\phi = 42$. Trace 1 is for flow at the treatment lip. Traces 2-5 are at greater depths (i.e., increments of 6.5 m).**
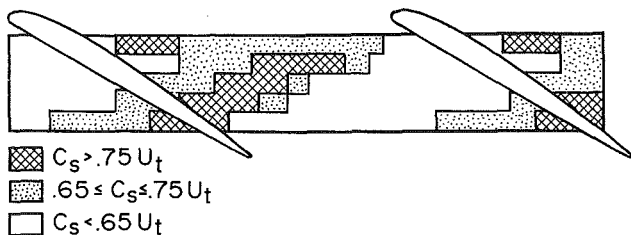


$\boxtimes$ $C_s > .75\,U_t$
$\square$ $.65 \leq C_s \leq .75\,U_t$
$\square$ $C_s < .65\,U_t$

**Fig. 21 Qualitative representation of the velocity of the flow in the treatment slots, $\phi = 0.42$**



**Fig. 22 Steady-state static pressure on the lip and at the base of the treatment slots, $\phi = 0.42$**

flow in the slot was obtained with a shielded hot-wire technique, described in [15], and these results are shown in Fig. 18 on a developed plant view of the treated outer annulus wall. Slightly more than one blade pitch is shown and the data refer to a position at mid-depth within the slot. Flow is seen to enter the cavities over approximately the downstream 60 percent of the slot and to leave the slot over approximately the upstream 20 percent of the slot. Both these findings apply to the entire blade passage. Some change in flow direction with time was detected using the hot-wire technique. The unsteadiness in flow angle was determined qualitatively and in the most extreme case was estimated at 15 deg. It must be stressed that the flow was therefore never observed to change sense, i.e., to enter the slot from a point where it had previously been emerging. The unsteadiness in direction was greatest near the front of the slot as the suction surface of the blade passed over it and near the rear at approximately blade midpassage. The magnitude of the velocity in the slot was
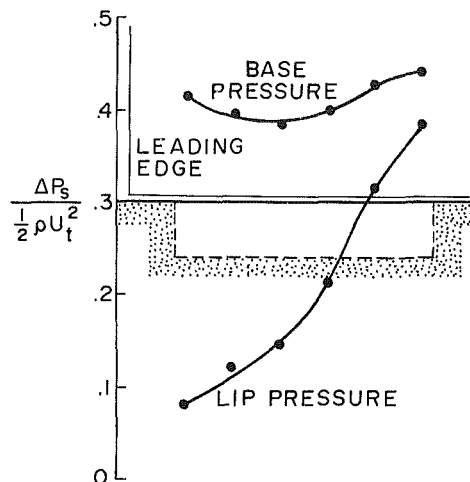
measured at 24 percent (6.5 mm) depthwise intervals within the slot and ensemble averaged over 80 rotor revolutions. The last measurement station was 1 mm from the base of the slot. The results of Fig. 19 were measured 5 mm downstream from the leading edge of the slot, whilst Fig. 20 were measured 5 mm upstream from the trailing edge of the slot, both at $\phi = 0.42$. It will be recalled that these positions correspond to areas where flow emerges from and enters the slot, respectively. In both cases six vertical lines have been overlaid to indicate the position of the pressure and suction surfaces of the blades of just over two blade passages. The shading represents the blade thickness. The largest velocities with the greatest level of fluctuation are found on the lip, but this reflects the movement of the blade more than transport inside the passage and is therefore less interesting. At the front and back of the treatment the flow has a nonzero mean, superimposed on which is a fluctuating velocity component at blade passing frequency. The velocity pattern does not vary significantly from one passage to another. Both the steady and unsteady components diminish rapidly as the base of the slot is approached.

The velocity fluctuation inside the slot shown in Figs. 19 and 20 is complicated and not fully explainable. It seems very probable that it is not of first importance, the main effect being the mean transport of the fluid from the back to the front. Near the rear of the slot the flow into the slot 6.5 mm below the tip shows a pronounced peak just before the pressure side of the blade crosses it. There is, however, no corresponding peak near the front of the slot, yet being a low Mach number flow one might expect the effects to travel with negligible delay. The explanation is that much of the fluctuation observed is rotational in nature and is, to first order, convected by the mean flow. This is made rather clearer in Fig. 21 where shading is used to indicate levels of velocity 6.5 mm below the lip. The peaks in the velocity drift to the right, relative to the blades, so that a line joining the peaks would be at about 55 deg to the axial. This angle is in fact calculated if the flow inside the slots that carries the disturbance upstream is equal to 0.7 times blade speed.

At $\phi = 0.36$, close to stall for the treated compressor, the velocity pattern inside the slots was basically the same, but rather larger in magnitude.

The time-mean static pressure at the lip and base of the slot are shown in Fig. 22 superimposed on a sketch of an axial section through the blade and the casing treatment. The case shown is for $\phi = 0.42$, but the results for other flow rates are similar. The pressure on the lip reflects a local pitchwise
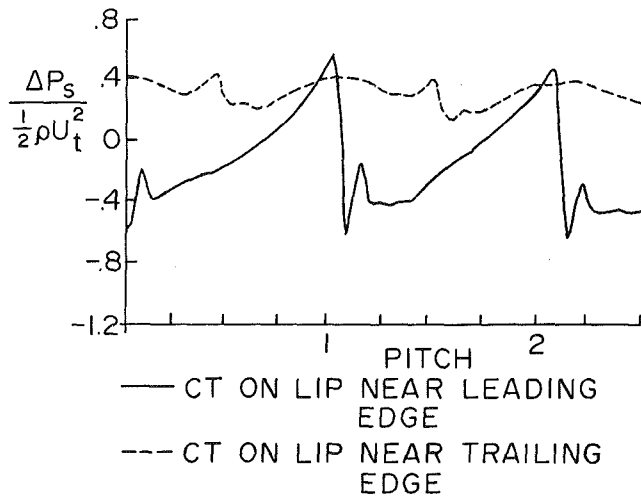
Fig. 23 Transient static pressure distribution on the lip of the treatment, $\phi = 0.42$

- CT ON LIP NEAR LEADING EDGE
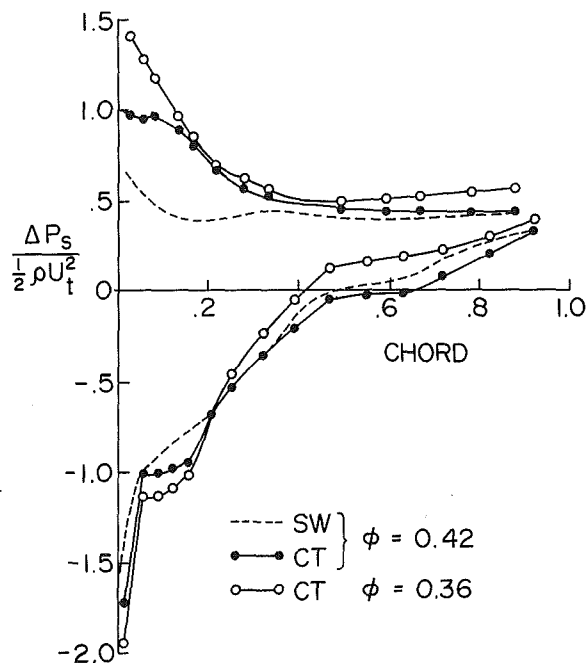--- CT ON LIP NEAR TRAILING EDGE



Fig. 24 Static pressure distribution on the rotor blades surface 6 mm from the outer annulus wall of the solid wall and treated rotors

average of the blade pressure field and consequently rises fairly uniformly from front to back. The pressure at the base of the slot is almost uniform and consistently higher than that at the tip. Thus where the flow enters the slot (over the rear 60 percent), the flow enters against an adverse pressure gradient. The process could, of course, be described differently by saying that the flow entering and being decelerated establishes a pressure gradient. The flow leaving near the front of the slot is accelerated out by a quite large pressure difference. The pressure difference does not help one to decide whether flow should be entering or leaving the slot and one therefore is forced to conclude that it is the direction of the flow near to the wall which determines this. As Fig. 15 shows, the absolute flow direction over the rear part of the treatment favors the flow entering. Without casing treatment, Fig. 13, the flow inclination close to the wall is such that it would enter treatment slots, if they were installed, at all axial stations. This raises the questions of why the flow configuration establishes itself in the way it does. One could imagine a

casing treatment gradually opening up under a flow previously established as in Fig. 13. In this case, one would expect the flow to be less successful at entering near the front, because of the much larger pressure difference between lip and base. From this, a circulatory pattern could be established with flow entering at the back and leaving, with rather higher absolute velocity, near the front. This has accepted a more or less constant pressure along the base of the slot, which is feasible since the geometry does not lend itself to large accelerations in the axial direction. The discussion of the pressure distribution in the slot is necessarily rather intuitive because of the complicated flow, even on a mean or steady basis. In addition, the velocity measurements have shown the flow to be strongly nonuniform and rotational and one side of the passage is exposed to a nonuniform pressure across which is a high velocity nonuniform flow.

The nonsteady pressure measurements in the treatment show varying pressure with time but with the base pressure generally higher than on the lip, see [15]. Near the rear of the treatment the lip pressure was found to be briefly higher than that at the base just before the blade pressure face passes over the slot. Under such circumstances the flow can enter the slots particularly easily and the observed peak in velocity can be seen in Fig. 20.

Figure 23 shows the pressure traces of the casing treatment lip near the leading and trailing edges. The comparative uniformity of the pressure near the rear of the treatment is striking. The pressure varies strongly near the treatment leading edge and in overall terms this variation is similar with and without casing treatment. The most interesting difference that the casing treatment produces is the peak in pressure evident just past the blade suction surface. It is conjectured that this is where the swirl induced by the rotor interacts with the swirl from the casing treatment with the consequent net deceleration producing a rise in pressure. Although of general interest, this does not appear to be of importance.

The pressure distributions around the tips of the rotor are shown in Fig. 24 for three different cases. There is the smooth wall and the casing treatment builds at $\phi = 0.42$ and the casing treatment close to its stall point at $\phi = 0.36$. The general shape and included area are very similar to that further from the tip, i.e., outside the annulus boundary layer, except for the high pressure near to the pressure side leading edge. This effect is produced by the flow leaving the treatment slots and is therefore fairly local to the tip. The suction side does show abrupt changes in slope, with flat regions of low gradient, suggesting separation and reattachment. This is most clear about 10 percent chord for the casing treatment at $\phi = 0.42$, but a similar effect may be present at about 50 percent. There does not appear to be any evidence of substantial separation or blade stall, consistent with the velocity vectors in Fig. 11 and Fig. 14.

## Concluding Remarks

Despite the measurements made it must be admitted that the reason for the effectiveness of casing treatment is not really understood. Fundamentally it is the ignorance regarding the precise flow mechanism leading to stall that makes this impossible. One can easily see that the rapid growth of blockage is enough to reduce the pressure rise–flow rate gradient and initiate instability, but the significance of this blockage occurring near the pressure surface is not clear.

At one level, the behavior of casing treatment seems very simple. A route is provided for flow to pass from the pressure surface to the suction surface so that a small proportion of the flow can be recirculated. The subtlety of a successful treatment like the axial skewed slot appears twofold. The boundary layer fluid tends to have high absolute swirl and therefore is suitably oriented to enter the treatment. Whereas the high

swirl velocity would be wasted in a normal smooth walled compressor, the casing treatment is capable of turning it and reintroducing it in a way which is utilizable. The casing treatment therefore selects the flow that is contributing to the blockage and then makes what would be a waste, useful. There does not seem to be any evidence other than the linear cascade flow visualization experiment described by Mikoljczak and Pfeffer [5] to suggest that aspirating the incipient or actual separation on the suction side contributes to the stall margin improvement. One can go further and say that the overwhelming trend for those casing treatments that do bring about stall margin improvement is the provision of a flow path between the pressure and suction surface. This would include circumferential grooves and blade angle slots.

The experiment by Greitzer et al. [4] can be interpreted in terms of our present tentative model. According to this, a stall margin improvement (and indeed improvement in pressure rise) due to casing treatment is only to be expected if the blading is such as to cause flow blockage to collect on the pressure surface. The high solidity blading used by Greitzer does this (see Fig. 8 of [4]) but the low solidity build does not since the low relative total pressure flow then collects in the suction surface/endwall corner. Within the usual meaning of the term the separation or stall is in the tip region for both solidities.

The present measurements have brought us to the tentative conclusion that unsteady effect in the slots are of minor importance: it is the steady or mean flow which matters. The processes in the region where the flow leaves the slot and interacts with the flow in the blade passage seems to be important, interesting, and poorly understood. One would like to know what is the optimum direction for the flow to leave the slots; it is certainly not clear that zero axial velocity and inclined to the radial at 60 deg is ideal. Short of an extensive "cut and try" exercise, this requires an understanding of the processes after the flow leaves the slot. The most obvious requirement appears to be more and better measurements in the blade passage, perhaps using rotating probes, laser measurement techniques or keeping the blade passage stationary and rotating the treatment. The latter approach was used by Takata and Tsukuda [2] and greatly simplifies the instrumentation for a minor sacrifice in flow realism.

If the axial skewed slot serves to remove blockage from the pressure surface/endwall corner and return it, turned through 180 deg, near the blade leading edge, one must remark that the rectangular geometry of the slots used is most peculiar. It is our belief that a continuously curved passage, perhaps semicircular, could be both more effective and easy to manufacture.

Because the rig used for these tests was not fitted with a torque meter it was impossible to find the loss in efficiency with casing treatment. The present experiments were unable to allow any useful conclusions to be drawn about the reasons for the loss of efficiency measured elsewhere when casing treatment has been used. It is proper to add that the cause of inefficiency in even smooth walled compressors is not understood; the sum of the profile loss, endwall boundary layer, and secondary flow is not sufficient to explain the observations, and improperly understood processes, notably those related to tip clearance flow, are probably crucial. The casing treatment might be expected to reduce the loss, by selectively removing the high loss fluid, but for reasons not explained this appears to be overwhelmed by one or more other effects.

It has been found [1] that the inclusion of a baffle half the axial distance along the casing treatment reduces the efficiency penalty whilst retaining most of the stall margin improvement. At first sight, this appears to conflict with the present conclusion that it is mean flow from the rear to the front that is basis of the stall margin improvement. This is not, however, the case. With highly staggered thin blades, such as those used in most modern compressors, and with casing treatment of typical axial length, there is ample opportunity for axial flow to occur from the pressure surface to the suction surface of the blades. The smaller efficiency penalty with this geometry probably points to undesirable levels of axial flow, or the inclusion of fluid which does not have high losses, when a baffle is absent. Still there remain many aspects that are either poorly understood or not understood at all.

## Acknowledgment

## References

1 Prince, D. C., Jr., Wisler, D. A., and Hilvers, D. E., "Study of Casing Treatment Stall Margin Improvement Phenomena," NASA CR-134552, Mar. 1974.

2 Takata, H., and Tsukuda, Y., "Study on the Mechanism of Stall Margin Improvement of Casing Treatment," ASME Paper No. 75-GT-13, ASME Gas Turbine Conference, Mar. 1975.

3 Camarata, F. J., Greitzer, E. M., Joslyn, H. D., and Nikkanen, E. P., "Effect of Casing Treatment on the Near Tip Flow Field of a Large-Scale Rotor," United Technologies Research Publication R7512136683-1, Dec. 1975.

4 Greitzer, E. M., Nikkanen, J. P., Haddad, D. E., Mazzawy, R. S., and Joslyn, H. D., "A Fundamental Criterion for the Application of Rotor Casing Treatment," ASME Journal of Fluids Engineering, Vol. 101, June 1979, pp. 237-24.

5 Mikolajczak, A. A., and Pfeffer, A. M., "Methods to Increase Engine Stability and Tolerance to Distortion," AGARD LS No. 72, Distortion Induced Instability.

6 Osborn, W. M., Lewis, G. W., Jr., and Heidelberg, L. J., "Effect of Several Porous Casing Treatments on Stall Limit and on Overall Performance of an Axial-Flow Compressor Rotor," NASA TN D-6537, Nov. 1971.

7 Moore, R. D., Kovich, G., and Blade, R. J., "Effect of Casing Treatment on Overall and Blade-Element Performance of a Compressor Rotor," NASA TN D-6538, Nov. 1971.

8 Fabri, J., and Reboux, J., "Effect of Outer Casing Treatment on Stall Margin of a Supersonic Rotating Cascade," ASME Paper No. 75-GT-95, ASME Gas Turbine Conference, Mar. 1975.

9 Tesch, W. A., "Evaluation of Range and Distortion Tolerance for High Mach Number Transonic Fan Stages, Task IV Stage Data and Performance Report for Casing Treatment Investigations," Vol. 1, NASA CR-72862, May 1971.

10 Bailey, E. E., "Effect of Grooved Casing Treatment in the Flow Range Capability of a Single-Stage Axial Flow Compressor", NASA TM X-2459, Jan. 1972.

11 Horlock, J. H., and Lakhwani, C. M., "Propagating Stall in Compressors With Porous Walls," ASME Paper No. 75-GT-59, ASME Gas Turbine Conference, 75-GT-59, 1975.

12 Amann, C. A., Nordensen, G. E., and Skellenger, G. D., "Casing Modification for Increasing the Surge Margin of Centrifugal Compressor in an Automotive Turbine Engine," ASME Journal of Engineering for Power, Vol 97, July 1975, pp. 329-336.

13 Koch, C. C., "A Criterion for Stall," ASME JOURNAL OF ENGINEERING FOR POWER, Vol. 103, 1981, pp. 645-656.

14 Gregory-Smith, D. G., "Annulus Wall Boundary Layers in Turbomachines," Ph. dissertaion, University of Cambridge, 1970.

15 Smith, G. D. J., "Casing Treatment in Axial Compressor," Ph.D. dissertation, University of Cambridge, 1980.

16 Whitfield, C. E., Kelly, J. C., and Barry B., "A Three Dimensional Analysis of Rotor Wakes," Aeronautical Quarterly, 1972, pp. 285-300.

17 Lewis W. E., "Fixed Direction Probes for Aerodynamic Measurements," Proc. Instn. Mech Engrs., Vol. 180, pt. 3J.